

Zero-field electron–nuclear double resonance of Gd^{3+} in GaSe

S. S. Ishchenko, V. G. Grachev, S. M. Okulov, and A. A. Klimov

Institute of Semiconductors, Academy of Sciences of the Ukrainian SSR, Kiev

(Submitted 9 April 1987)

Zh. Eksp. Teor. Fiz. **93**, 2102–2108 (December 1987)

An electron–nuclear double resonance (ENDOR) has been recorded and investigated in zero magnetic field. The experiments were carried out on Gd^{3+} centers in a layer crystal of GaSe. Theoretical expressions have been obtained for the spectrum of zero-field ENDOR. A comparison of the theory and experiment yields the parameters of the hyperfine and quadrupole interactions of the gallium nuclei located near a defect. An anomalously high intensity of “forbidden” nuclear transitions ($\Delta\tilde{m} = \pm 2, \pm 3$) was observed, which can be explained by a fast relaxation process characterized by $\Delta M = \pm 1$ and $\Delta\tilde{m} = \pm 2$ and participating in the ENDOR mechanism. The experimental results indicate that the zero-field ENDOR signal of polycrystalline GaSe is identical with the signal of a single crystal. The orientation of oscillatory fields in zero-field ENDOR has been studied. The experimental results and the general advantages of zero-field ENDOR are analyzed.

INTRODUCTION

Zero-field (observed in zero magnetic fields) electron^{1,2} and nuclear^{3,4} spin resonances have been investigated both theoretically and experimentally and are now being used in rf spectroscopy providing “clean” data on the interaction of electron and nuclear spins with internal crystal fields and with one another. The most effective technique for investigating resonance absorption by nuclei located near paramagnetic centers is the electron–nuclear double resonance (ENDOR) method^{5–7} in which transitions between nuclear spin sublevels are manifested by a change in the intensity of a saturated ESR signal. An external static magnetic field used in ENDOR spectrometers plays an important role in producing the signal (in the ENDOR mechanism) and largely determines the resonance frequencies in the spectrum. It is not *a priori* clear whether it is at all possible to observe an ENDOR signal in zero magnetic field. This is because this signal appears only for specific ratios of the relaxation times in the electron–nuclear system. In zero magnetic fields such a ratio may be unfavorable for ENDOR studies.

We shall report observations of zero-field ENDOR recorded for Gd^{3+} centers in a GaSe crystal. A theoretical description of the zero-field ENDOR spectrum will be presented and its characteristics will be discussed. Information capabilities of zero-field ENDOR will be discussed and its advantages compared with ENDOR in strong magnetic fields and with single-frequency zero-field resonances will be considered.

EXPERIMENTS AND THEORETICAL DESCRIPTION

We recorded ENDOR spectra in the absence of a static magnetic field in a sample kept at liquid helium temperature. This was done using an ÉYa-1301 superheterodyne ENDOR spectrometer working in the 3-cm range of wavelengths. This spectrometer contained a cylindrical microwave cavity resonator supporting the H_{011} oscillation mode, whose frequency could be tuned by moving a plunger. An rf field inducing nuclear transitions was generated by four rods driven across the resonator cavity parallel to its axis and connected in accordance with the Helmholtz scheme.

We investigated GaSe layer crystals containing gadolinium as an impurity, which were grown by the Bridgman method and had the structure of the ϵ polytype (space symmetry group $P\bar{6}m2$). Gadolinium formed a set of paramagnetic centers in these crystals.⁸ We observed zero-gap ENDOR for a Gd^{3+} center (electron spin $S = 7/2$) replacing (without charge compensation in the immediate environment) a covalent-bound pair Ga_2^{4+} of the kind containing selenium atoms from the neighboring layers as the nearest neighbors along the optic axis c . The ESR spectrum of the center consisted of seven lines and in a magnetic field $H\parallel z$ can be described by the Hamiltonian

$$\mathcal{H}_{\text{ESR}} = g\beta HS_z + V_0^2 V_0^2 (S) \quad (1)$$

with $g = 1.989 \pm 0.001$ and $V_0^2 = -1177 \pm 1$ MHz. Here and later we shall use the crystallographic coordinate system $z\parallel c\parallel \bar{6}$, $x\parallel m$, $y\parallel 2$, and the notation of Refs. 9 and 10, where V_0^2 is an orthonormalized spin operator.

If $H = 0$, then the $M = \pm 5/2 \leftrightarrow \pm 7/2$ transition (M is the projection of the electron spin along the z axis) lies in the 3-cm range of wavelengths. This made it possible to use our apparatus to record resonance absorption of zero-field ESR. Observation of zero-field ENDOR involved recording zero-field ESR at one of the points of a resonance line (for example, at its maximum) without frequency scanning of the whole ESR line.

The frequency of the oscillations corresponding to the splitting of the electron spin levels in zero magnetic field was determined by recording the resonance magnetic field of the ESR line, observed near $H = 0$, as a function of the microwave source frequency H_r (ν_{micr}), as shown in Fig. 1. The part of this dependence to the right of the minimum corresponded to the transition $M = -5/2 \leftrightarrow -7/2$ and that to the left of the minimum corresponded to $M = +5/2 \leftrightarrow +7/2$. The dependence was recorded as follows. The ESR line was obtained by scanning the magnetic field and determining its resonance value. Then, the microwave source frequency was reduced by a certain amount and the resonator frequency was adjusted using the plunger so that it coincided with the microwave source frequency; the ESR line profile was recorded again. The residual field of the elec-

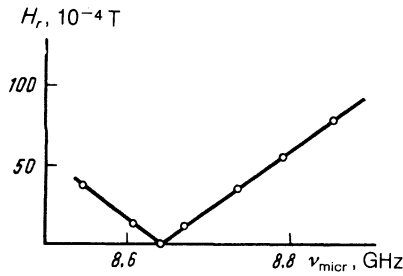


FIG. 1. Dependences of the resonance magnetic field H_r for $\pm 5/2 \leftrightarrow \pm 7/2$ on the frequency ESR transitions of the source of the microwave field.

tromagnet was compensated by an oppositely directed magnetic field created by additional coils.

A microwave quantum corresponding to the minimum of the dependence $H_r(\nu_{\text{micr}})$ was exactly equal to the splitting of the levels in zero field. It was this frequency, amounting in our case to 8646 MHz, which was used to record zero-field ENDOR. This was followed by saturation of the electron spin transition and exposure of the sample to an amplitude-modulated rf field (modulation frequency ~ 1 kHz). An increase in the intensity of the saturated absorption signal of zero-field ESR at the moment when the rf field induced nuclear spin transitions was recorded by the lock-in detection method at the modulation frequency, representing the steady-state zero-field ENDOR signal. These transitions were excited by the magnetic components of the microwave and rf fields and their vectors \mathbf{H}_1 and \mathbf{H}_2 , respectively, were perpendicular to one another and to the c crystal axis.

Such zero-field ENDOR signals were obtained for the 12 gallium nuclei closest to Gd^{3+} (nuclear spin $I = 3/2$), which were located in the same layer as an impurity ion and separated from this ion by the same distances.¹¹ In the case of zero-field ENDOR all these nuclei became identical in rf spectroscopy, in contrast to ENDOR in a magnetic field, so that the signals could simply be added. Figure 2 shows the zero-field ENDOR spectrum obtained for the nuclei of the ^{69}Ga isotope. A similar spectrum was recorded for the ^{71}Ga nuclei. The optimal directions of the oscillatory fields in zero-field ENDOR were determined and additional information on the rf spectroscopic parameters was obtained by investigating the orientational dependence of the signal intensities. An example of this dependence is plotted in Fig. 3. All the observed dependences had a maximum for \mathbf{H}_1 and \mathbf{H}_2 , both perpendicular to c .

The ENDOR spectra were described by an effective spin Hamiltonian⁹

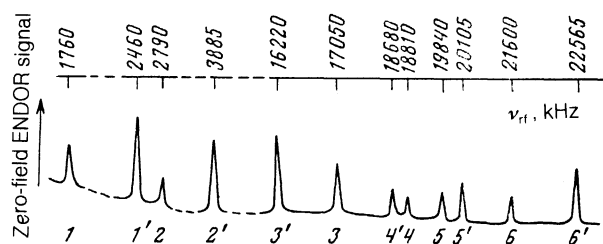


FIG. 2. Zero-field ENDOR spectrum of the ^{69}Ga nuclei located near the Gd^{3+} ions in a GaSe crystal. The lines are labeled in the same way as the transitions in Fig. 4.

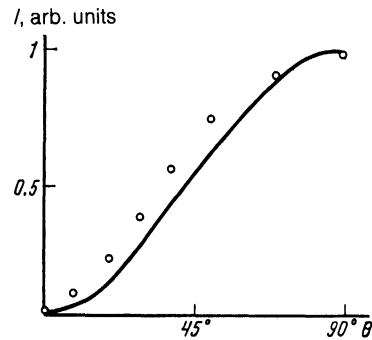


FIG. 3. The intensity of the zero-field ENDOR signal in the case of the $-3/2 \leftrightarrow -1/2$ nuclear transition as a function of the orientation of the rf field. Here, θ is the angle between \mathbf{H}_2 and the z axis. The signal includes contributions of 12 magnetically inequivalent gallium nuclei and the intensity of the signal is independent of the azimuthal angle. The continuous curve represents the theory [Eq. (4)] and the points are the experimental results.

$$\mathcal{H}_{\text{ENDOR}}^M = \sum_n q_n^2 V_n^2(I) + M \sum_p A_{zp} I_p, \quad (2)$$

$$n=0, \pm 1, \pm 2, \quad p=x, y, z,$$

where q_n^2 and A_{zp} are the quadrupole and hyperfine parameters; $\langle M |$ is the eigenfunction of Eq. (1) for $H = 0$.

The formulas obtained with the aid of Eq. (2) in the $A_{zp} \gg q_n^2$ approximation could not describe the observed spectra. We assumed that $q_0^2 \gg A_{zp}$ and $q_0^2 \gg q_n^2 \neq 0$, and allowed for the degeneracy of levels in the zeroth approximation of perturbation theory, which gave the following expressions for $I = 3/2$:

$$E_{\pm 3/2}^M = q \pm^3 / 2 M A_{zz} + t_{\pm}^M + u_{\mp}^M, \quad (3)$$

$$E_{\pm 1/2}^M = -q \pm M (A_{xx}^2 + A_{yy}^2 + A_{zz}^2 / 4)^{1/2} - t_{\pm}^M - u_{\pm}^M,$$

$$q = q_0^2 (3/2)^{1/2}, \quad t_{\pm}^M = |\alpha (d \pm M f) + \beta c|^2 / 2q,$$

$$u_{\pm}^M = |\alpha c^* - \beta d^* \pm M \beta f^*|^2 / 2q,$$

$$\left\{ \begin{array}{l} \alpha \\ \beta \end{array} \right\} = \left[\frac{A_{ix} \pm i A_{iy}}{2(A_{ix}^2 + A_{iy}^2)^{1/2}} \left(1 \pm \frac{A_{zz}}{[A_{zz}^2 + 4(A_{ix}^2 + A_{iy}^2)]^{1/2}} \right) \right]^{1/2},$$

$$c = \frac{3}{\sqrt{2}} (q_2^2 - i q_{-2}^2), \quad d = 3\sqrt{2} (q_1^2 - i q_{-1}^2),$$

$$f = \frac{1}{2} (A_{ix} - i A_{iy}) \sqrt{3}.$$

The energy levels described by the system (3) are shown schematically in Fig. 4. The vertical lines are the nu-

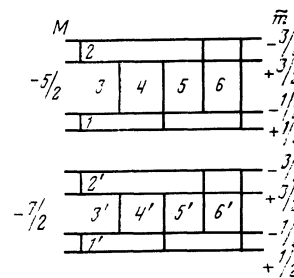


FIG. 4. Spin energy levels of the Ga nucleus shown allowing for the hyperfine and quadrupole interactions on the assumption that $M = -5/2$ and $-7/2$, and \tilde{m} is the quantum number with the values $\pm 1/2$ and $\pm 3/2$. If $M = +5/2$ and $+7/2$, then the values of \tilde{m} in this figure should be replaced by values with the opposite sign.

clear transitions corresponding to the experimentally observed resonance lines (Fig. 2). The transition probabilities, to which the line intensities were proportional, were calculated using the same approximations as for the system of equations (3) and this was done for each of the 12 nuclei (which were inequivalent in relation to \mathbf{H}_2); this was followed by summation. In the case of the transition shown in Fig. 4, we obtained

$$J_1 = \frac{4}{3} J_0 \left\{ |\alpha|^4 + |\beta|^4 + |\alpha\beta|^2 \operatorname{tg}^2 \theta + \frac{\sqrt{3}}{2q} [(\alpha\alpha^* - \beta\beta^*)(\alpha\beta^*d^* - \alpha^*\beta d) + (\alpha^2\beta^2 + \alpha^2\beta^{*2})(c+c^*)] \right\},$$

$$J_2 = J_0 |c/q|^2, \quad J_{3,6} = J_0 (\beta\beta^* - \gamma_{\pm}), \quad J_{4,5} = J_0 (\alpha\alpha^* + \gamma_{\pm}), \quad (4)$$

where

$$J_0 = \frac{1}{2} (g_n \beta_n H_2)^2 \sin^2 \theta,$$

$$\gamma_{\pm} = [\alpha\beta^*(d^* \pm Mf^*) + \alpha^*\beta(d \pm Mf)] / q\sqrt{3}. \quad (5)$$

Since the factors governing the intensities of zero-field ENDOR lines (such as relaxation times, amplitudes of the fields \mathbf{H}_1 and \mathbf{H}_2 , etc.) added to the probabilities of Eqs. (4) and (5) a factor independent of the angle θ between \mathbf{H}_2 and z , the angular dependences of the line intensities (in arbitrary units) were described satisfactorily by Eqs. (4) and (5).

One could show, by analogy with Ref. 10, that the energy levels of Eq. (3) are characterized by nonseparable combinations of the parameters whose number is less than the number of parameters in Eq. (2). However, a comparison of the experimental frequencies and dependences of the line intensities on θ provides an opportunity to determine the full set of parameters of Eq. (2). In our case the positions of the ENDOR lines of the ^{69}Ga nuclei (within the limits of an experimental error of ± 5 kHz) and the angular dependences of the line intensities (to within 15%) were described by assuming $A_{zz} = 370.7 \pm 0.2$, $A_{xx} = 375.5 \pm 1$, $q_0^2 = 7658 \pm 10$, $q_2^2 = 1018 \pm 20$, and $A_{zy} \approx q_{\pm 1}^2 \approx q_{-2}^2 \approx 0$ (all these quantities are given in kilohertz). The ratio of the parameters of the ^{69}Ga and ^{71}Ga nuclei agreed with the tabulated ratios of their magnetic and quadrupole moments.

The following experimental observations should be noted. Zero-field ENDOR enabled us to record all the nuclear transitions possible in the system of energy levels of Eq. (3). The anomalously high intensity of the transitions with $\Delta\tilde{m} = \pm 3$ and ± 2 (lines 2, 2', 3, 3', 6, and 6' in Fig. 2) is noteworthy; in strong magnetic fields these transitions would normally be forbidden. The width of the zero-field ENDOR lines was 50 ± 5 kHz and it was unaffected by going over to ENDOR in a finite magnetic field. We also observed zero-field ENDOR in polycrystalline GaSe:Gd samples. Their resonance spectra were identical with the spectra of single crystals.

DISCUSSION OF RESULTS

The ENDOR of the investigated centers was recorded first in Ref. 8 in a magnetic field $\mathbf{H} \parallel \mathbf{c}$. However, in view of the complexity of the spectrum (characterized by the presence of additional line splitting due to inaccurate orientation of \mathbf{H} and imperfections of the crystal) and also because of difficulties encountered in theoretical analysis for one orientation of the magnetic field, we were unable to identify com-

pletely the ENDOR lines due to the gallium nuclei and to describe them theoretically in Ref. 8. Simplification of the spectrum and its analysis involving avoidance of the Zeeman interaction made it possible to tackle this task using zero-field ENDOR. All the ENDOR lines were attributed to specific nuclear transitions and the parameters representing the hyperfine and quadrupole interactions of the gallium nuclei nearest to Gd^{3+} were determined.

A comparison of our quadrupole interaction parameters with nuclear quadrupole resonance data¹² for undoped GaSe indicated a relatively small (less than 3%) change in the internal crystal field gradient of the gallium nuclei when Gd^{3+} was located close to it. This, together with the observation that the measured hyperfine interaction parameters of these gallium nuclei were small, of the order of the parameters of the dipole-dipole interaction of electron and nuclear spins, demonstrated a strong localization of the wave function of Gd^{3+} and a slight perturbation of the crystal lattice by this ion.

In the case of a conventional magnetic resonance the signal is maximal when the oscillatory field exciting the transitions is directed at right-angles to a static magnetic field. In the case of zero-field resonances, and particularly in the case of zero-field ENDOR, the optimal orientation of the oscillatory fields is more complex and it depends on the ratio of the various interaction in a system and on their directions. In the case when one interaction predominates, so that it governs the quantization axis of spins, an oscillatory field should be directed at right-angles to this axis. The maxima we recorded in the dependences of the intensities of the zero-field ENDOR lines obtained in the $\mathbf{H}_2 \perp \mathbf{c}$ orientation were due to the fact that the longitudinal component of the quadrupole interaction tensor was much greater than the other parameters. Although it was not possible to determine all the parameters of the spin Hamiltonian simply by analyzing the resonance frequencies of low-symmetry systems, the necessary additional information was deduced from the dependences of the signals on the orientations of the fields \mathbf{H}_1 and \mathbf{H}_2 .

The probabilities of the nuclear transitions $\Delta\tilde{m} = \pm 2, \pm 3$ [see Eqs. (4) and (5)] were nonvanishing due to the mixing of these states by the hyperfine interaction because of the large value of the parameter q_2^2 . The anomalously high intensities of the lines due to these transitions compared with those as a result of the $\Delta\tilde{m} = \pm 1$ transitions can be explained as follows. We recorded the steady-state ENDOR signal which appeared because the rf background, at the moment when the nuclear transitions were induced, activated not only the main channel of relaxation opposing microwave saturation (corresponding to transitions with $\Delta M = \pm 1, \Delta\tilde{m} = 0$), but also an additional relaxation channel with $\Delta M = 11$ and $\Delta\tilde{m} \neq 0$. Usually the $\Delta M = \pm 1$ and $\Delta\tilde{m} = \pm 1$ relaxation transitions were more effective than the $\Delta M = \pm 1$ and $\Delta\tilde{m} = \pm 2, \pm 3$ transitions. In our case, in all probability this ratio was reversed. This could be due to the presence of a local vibration of Gd^{3+} or due to the characteristics of the vibrational processes in a layer crystal.

However, the width of the resonance lines in finite-field and zero-field ENDOR indicated that there was no contribution to the broadening from the processes associated with the Zeeman interaction.

CONCLUSIONS

We now consider certain general features of zero-field ENDOR. The most important is in our opinion the fact that the zero-field signal ENDOR is entirely due to the magnetic hyperfine and electric quadrupole interactions, whereas in the case of the usual (finite-field) ENDOR signal these interactions are simply perturbing factors compared with the dominant Zeeman effect and, therefore, they cannot be always determined reliably with a high degree of precision against the background. Similar "clearing" of contributions associated with the Zeeman interaction in zero-field ENDOR occurred in the case of line widths, and also in relaxation processes governing the ENDOR mechanism. The characteristics of these processes could be obtained by investigating the dynamics of zero-field ENDOR.

One should mention particularly the feasibility of using zero-field ENDOR to investigate the electron-nuclear interactions in polycrystalline and amorphous bodies. The ENDOR method has not yet been applied to such systems, because the orientational broadening of the spectra made it difficult to observe ENDOR, the identification of the signals became more complex, and the data-carrying capacity deteriorated. However, the spectra of zero-field ENDOR due to polycrystalline samples should, by analogy with the spectra of single crystals, have the same line widths and should retain completely their data capacity. Consequently, it should be possible to investigate fine surface effects in solids by the ENDOR method.

The advantage of the zero-field ENDOR method compared with zero-field single-frequency resonances is above all the ability to obtain information on hyperfine and quadrupole interactions in solids near defects, i.e., information on the local properties of matter. Such information could not be obtained by the zero-field NMR method, because of its low sensitivity, or by the zero-field ESR method, because of insufficient resolution of the latter.

The advantages of the zero-field ENDOR method are as follows.

1. Simplification of the spectrum and increase of its intensity (compared with the finite-field ENDOR signal) because of disappearance of the multiplets in the signals due to the nuclei in the same coordinate sphere and the multiplets in ESR due to magnetically inequivalent centers.

2. The absence of effects of mosaic and block structures of crystals.

3. An increase in the resolution as a result of narrowing

of the resonance lines and an increase in the precision of the determination of the parameters because of the absence of errors associated with the magnetic field measurements.

4. Easier diagonalization of the spin Hamiltonian and contribution of the observed lines to specific nuclear transitions, which is an important factor in the ENDOR investigations of complex spin systems.

An important advantage of the zero-field ENDOR method from the technical point of view is the ability to use conventional spectrometers without any attachments. This makes these methods advantageous compared, for example, to zero-field ENDOR or zero-field ESR, but it is necessary to construct special apparatus which is not produced serially² and this is a serious difficulty in the extensive use of the latter. The above advantage makes it possible to combine readily measurements of zero-field ENDOR and of finite-field ENDOR, which should increase the information that can be obtained in this way.

The authors are grateful to A. B. Roitsin and B. D. Shanina for discussing the results.

¹L. S. Kornienko and A. M. Prokhorov, *Zh. Eksp. Teor. Fiz.* **40**, 1594 (1961) [*Sov. Phys. JETP* **13**, 1120 (1961)].

²R. Bramley and S. J. Strach, *Chem. Rev.* **83**, 49 (1983).

³A. Abragam, *The Principles of Nuclear Magnetism*, Clarendon Press, Oxford (1961).

⁴V. S. Grechishkin, *Nuclear Quadrupole Interactions in Solids* [in Russian], Nauka, Mvscow (1973).

⁵G. Feher, *Phys. Rev.* **103**, 500 (1956).

⁶A. Abragam and B. Bleaney, *Electron Paramagnetic Resonance of Transition Ions*, Clarendon Press, Oxford (1970).

⁷V. G. Grachev and M. F. Deigen, *Usp. Fiz. Nauk* **125**, 631 (1978) [*Sov. Phys. Usp.* **21**, 674 (1978)].

⁸A. A. Klimov, V. G. Grachev, S. S. Ishchenko, Z. D. Kovalyuk, S. M. Okulov, and V. V. Teslenko, *Fiz. Tverd. Tela (Leningrad)* **29**, 28 (1987) [*Sov. Phys. Solid State* **29**, 16 (1987)].

⁹M. D. Glinchuk, V. G. Grachev, M. F. Deigen, *et al.*, *Electric Effects in RF Spectroscopy* [in Russian], Nauka, Moscow (1981).

¹⁰V. G. Grachev, *Zh. Eksp. Teor. Fiz.* **92**, 1834 (1987) [*Sov. Phys. JETP* **65**, 1029 (1987)].

¹¹R. W. G. Wyckoff, *Crystal Structures*, 2nd ed., Vol. 3, Interscience, New York (1965).

¹²T. J. Bastow, I. D. Campbell, and H. J. Whitfield, *Solid State Commun.* **39**, 307 (1981).

Translated by A. Tybulewicz